Pole-Zero Modeling of Flexible Space Structures

Bong Wie
University of Texas at Austin, Austin, Texas
and
Arthur E. Bryson Jr.
Stanford University, Stanford, California

Generic models of flexible space structures are investigated from the infinite discrete-spectrum viewpoint of distributed parameter systems. The models are simple enough to treat analytically, yet complicated enough to demonstrate the practical usefulness of the transcendental-transfer-function modeling for the purposes of preliminary control synthesis. Transfer functions of the various generic models are derived analytically, and their pole-zero patterns are investigated. The alternating pole-zero pattern of a transfer function from an actuator to the colocated sensor is well-known. It is, however, newly found that in certain colocated cases, each mode has an associated zero of higher frequency than the pole; in fact, the rigid-body mode has an associated zero very close to the origin. This direct transmission property must be taken into consideration when designing large space structures such as the dual-keel Space Station, which has a pole-zero pattern very similar to that of the generic models. The practical significance of such pole-zero patterns on colocated control is discussed.

Introduction

LARGE space structures will consist of many lumped and truss-like subsystems with fairly complex interconnections. In certain cases, distributed parameter modeling of beam- and truss-like lattice structures[1-5] may be more computationally effective than conventional lumped- or discrete-parameter modeling using finite element methods. However, distributed parameter models need to be converted to finite-dimensional state space models or transfer function models for the purposes of control design. Consequently, the development of computer-aided methods for the frequency-domain modeling of hybrid systems with complex interconnections of lumped and distributed parameter subsystems is of current practical interest.[6-8]

In this paper, we investigate various generic models of flexible structures which are simple enough to treat analytically, yet complicated enough to demonstrate the practicality of frequency-domain modeling of hybrid systems. We emphasize the analytical modeling of simple hybrid systems for the purposes of parametric study in terms of their pole-zero patterns. Although controlling a flexible structure using many actuators and sensors is of interest to control researchers, we focus on the fundamental issue of controlling a flexible structure using one actuator and a colocated sensor.

When the actuator and sensor are colocated on a free-free structure, the transfer function has alternating poles and zeros along the imaginary axis.[9,10] In this case the rigid-body mode and all the structural modes are stably interacting with each other; consequently, all the modes can be phase-stabilized by

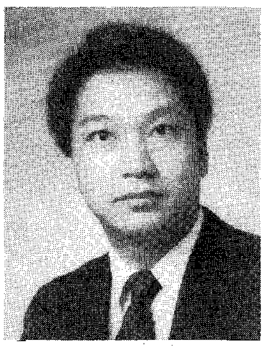

Bong Wie was born in Seoul, Korea, on February 25, 1952. He received a B.S. degree in aeronautical engineering from Seoul National University in 1975, and M.S. and Ph.D. degrees in aeronautics and astronautics from Stanford University in 1978 and 1981, respectively. From 1981 to 1985, he was employed as a Control/Dynamics Analyst at the Ford Aerospace & Communications Corporation. In 1985, he joined the faculty of the University of Texas at Austin where he is currently an Assistant Professor in the Department of Aerospace Engineering and Engineering Mechanics. His research interests include spacecraft control and dynamics, control systems synthesis, and modeling and control of large space structures. He is an Associate Editor for the *Journal of Guidance, Control, and Dynamics*. He is also a Member of the AIAA and is a consultant to the Ford Aerospace & Communications Corporation.

Arthur E. Bryson Jr. received a B.S. in aeronautical engineering from Iowa State University in 1946 and a Ph.D. in aeronautics from the California Institute of Technology in 1951. In 1953 he joined the faculty of Harvard University where he was appointed Professor in 1961. In 1968 he went to Stanford University where he was Chairman of the Department of Applied Mechanics (1969–1971) and of the Department of Aeronautics and Astronautics (1971–79); he was named Paul Pigott Professor of Engineering in 1972. He is author or coauthor of 110 technical papers on flight mechanics, automatic control, and fluid mechanics. He was Hunsaaker Visiting Professor at MIT in 1965–66 and chairman of the Aeronautic & Space Engineering Board of the NRC (1976–78). He is a Fellow of AIAA and a member of the National Acacemy of Engineering and the National Academy of Sciences.

Received May 11, 1987; revision received Aug. 3, 1987.

position feedback with a lead compensator or combined position and rate feedback. In practice, phase uncertainty from the control loop time delay and actuator/sensor dynamics must be considered in stabilizing all the flexible modes. In particular, the lowest zero of the transfer function (colocated case) needs special consideration, since the attitude control bandwidth is severely limited by the lowest zero if it is very close to the origin.

In this paper, generic hybrid models with simple interconnections of lumped and distributed parameter subsystems are investigated from the discrete-spectrum viewpoint. For these models, we show a unique pole-zero pattern, where each mode has an associated zero of higher frequency than the pole; in fact, the rigid-body mode has an associated zero very close to the origin. This results in a wide frequency spectrum which causes some difficulties in reducing the model order and also in roll-off filtering of the unmodeled higher frequency modes. If the last structural mode zero is included in the reduced-order model, then the reduced-order transfer function will have the same number of poles and zeros. This is quite different from most of the cases, where there are more poles and zeros (natural roll-off). However, it does not mean that the conventional modal truncation method gives improper results.

The practical significance of such pole-zero patterns of simple models is that a very similar pole-zero pattern can be found for the dual-keel Space Station[11] for which colocated control may not be a trivial problem, if a high bandwidth attitude control is required. Similar pole-zero patterns for simple beam- and rod-like structures have been examined using exact transfer functions.[12,13] The practical usefulness of this analytical frequency-domain modeling approach has been demonstrated in Ref. 14 for active vibration control synthesis of the COFS-I Mast Flight System. In this paper, we derive exact transfer functions of various simple hybrid models and examine their direct transmission characteristics. We then briefly discuss some practical control issues related to colocated control.

A Rigid Body with Beam-Like Appendages

In this section, we consider a rigid body connected with uniform Bernoulli-Euler beams as a generic model of a spacecraft with symmetric flexible appendages. This simple model has been used by control researchers, but we emphasize here the pole-zero patterns for different values of system parameters, such as the moment of inertia and the appendage length/mass. For a simplified single-axis case, as shown in Fig. 1, the linearized rotational equation of motion is

$$[EI\eta''(x,t)]'' + \sigma[(R+x)\ddot{\theta}(t) + \ddot{\eta}(x,t)] = 0 \quad (1)$$

and the boundary conditions are

$$J\ddot{\theta}(t) = u(t) - [2REI\eta'''(0,t)] + [2EI\eta''(0,t)] \quad (2a)$$

$$\eta(0,t) = \eta'(0,t) = 0 \quad (2b)$$

$$\eta''(l,t) = \eta'''(l,t) = 0 \quad (2c)$$

where $\theta(t)$ is the rotational angle of the central rigid body with respect to inertial reference frame; $\eta(x,t)$ is the small elastic deformation of the appendages with respect to the reference frame attached to the central rigid body; $u(t)$ is the control torque applied to the central rigid body; EI is the bending stiffness of the appendage; σ is the mass density per unit length of the appendage; l is the length of the single appendage; J is the rotational inertia of the central rigid body; R is the radius of the central rigid body; and the prime and dot denote partial differentiation with respect to x and t, respectively. The central body is assumed to be a sphere ($J = (2/5)MR^2$).

Equation (1) has a variable coefficient, but if we define a new coordinate $y(x,t)$ as

$$y(x,t) \triangleq [(R+x)\theta(t)] + [\eta(x,t)] \quad (3)$$

then we have a simple uniform beam equation (with constant coefficient)

$$[EIy''''(x,t)] + [\sigma\ddot{y}(x,t)] = 0 \quad (4)$$

and the boundary conditions in terms of the new coordinate $y(x,t)$

$$J\ddot{\theta} = u(t) - [2REIy'''(0,t)] + [2EIy''(0,t)] \quad (5a)$$

$$\theta(t) = y'(0,t) \quad \text{and} \quad y(0,t) = Ry'(0,t) \quad (5b)$$

$$y''(l,t) = y'''(l,t) = 0 \quad (5c)$$

Taking the Laplace transforms of Eqs. (4) and (5), it is straightforward to derive the transcendental transfer function from control torque $u(s)$ to attitude angle $\theta(s)$ of the central rigid body

$$\frac{\theta(s)}{u(s)} = \frac{N(s)}{D(s)} \quad (6)$$

where

$$N(s) \triangleq -(1 + c\lambda ch\lambda)$$

$$D(s) \triangleq 2\lambda[(1 + P_1\lambda^2)ch\lambda s\lambda + (P_1\lambda^2 - 1)sh\lambda c\lambda + 2P_1\lambda sh\lambda s\lambda + (2/5)P_1^2P_2\lambda^3(1 + c\lambda ch\lambda)]$$

$$sh(\lambda) \triangleq \sinh(\lambda),\ ch(\lambda) \triangleq \cosh(\lambda),\ s(\lambda) \triangleq \sin(\lambda),$$

and

$$c(\lambda) \triangleq \cos(\lambda)$$

and $\lambda^4 \triangleq -s^2$, s in units of $[EI/\sigma l^4]^{\frac{1}{2}}$ and $u(s)$ in units of EI/l.

The dimensionless structural parameters are defined as

$$P_1 = \frac{R}{l} = \frac{\text{radius of spherical central body}}{\text{lenght of single appendage}}$$

$$P_2 = \frac{M}{2\sigma l} = \frac{\text{mass of central rigid body}}{\text{total mass of two appendages}}$$

The vanishing of the numerator of Eq. (6) is identical to the characteristic equation of a cantilevered beam of length l. Thus, the zeros of the transfer function [Eq. (6)] are identical to the natural frequencies of a cantilevered beam.

For the special case without the central body, Eq. (6) becomes

$$\frac{\theta(s)}{u(s)} = \frac{1 + c\lambda ch\lambda}{2\lambda(sh\lambda c\lambda - ch\lambda s\lambda)} \quad (7)$$

which corresponds to the transfer function of a free-free beam of length $2l$, with control torquer and rotational angle sensor at the center of the beam.

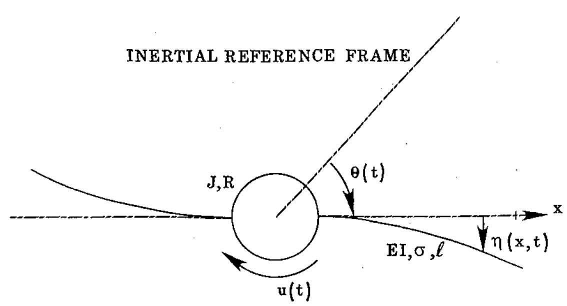

Fig. 1 A rigid body with beam-like appendages.

The pole-zero patterns of Eq. (6) for different values of P_1 and P_2 are shown in Fig. 2. As expected, the poles and zeros alternate along the imaginary axis, and the pole-zero pairs of each vibration mode depend on the structural parameters P_1 and P_2. For a free-free beam without the central rigid body each pole has an associated zero of higher frequency than the pole, and the lowest zeros are very close to the origin. As we increase the moment of inertia of the central rigid body, the poles become associated with a zero of lower frequency, and the vibration modes become nearly uncontrollable (undisturbable) and unobservable by the control torquer and the attitude angle sensor at the central rigid body.

The significance of co-location of actuator and sensor is that the transfer function has alternating poles and zeros. All of the modes can then be stabilized by using a direct angle and rate feedback in an ideal case with no extra control loop dynamics. It is, however, interesting to consider the closed-loop behavior of a colocated system by examining the root locus vs rate feedback gain for the exact infinite-dimensional model. Consider a special case without the central rigid body, which might be a very large beam-like structure with negligible rigid body section. It is clear from Fig. 3 that each pole has an associated zero of higher frequency than the pole, and that the higher frequency modes have more control/structure interactions than the lower frequency modes. We also see that the rigid body pole at the origin moves to the left, meeting a pole coming from infinity. They then break out of the real axis and move toward the first set of zeros. The physical significance of this result is that the direct rate feedback for a system with a direct transmission characteristic needs special consideration. This will be further discussed later.

Next, we investigate a flexible frame as well as a rigid frame with a pretensioned membrane, which might be simple analytical models of the large solar arrays of the Space Station.[11] The effect of membrane tension on the pole-zero pairs of vibration modes is also investigated. It is shown that reduced-order models of the flexible frame with a pretensioned membrane may have the same number of poles and zeros; that is, they may be characterized as a dynamic system with a direct transmission term in the transfer function with colocated actuator and sensor pair.

Rigid Frame with a Pretensioned Membrane

A simplified model of a membrane-type solar array is shown in Fig. 4. The solar array (or blanket) is pretensioned in one direction, and may be described by the wave equation

$$z''(x,t) - [(\rho_0/T_0)\ddot{z}(x,t)] = 0 \tag{8}$$

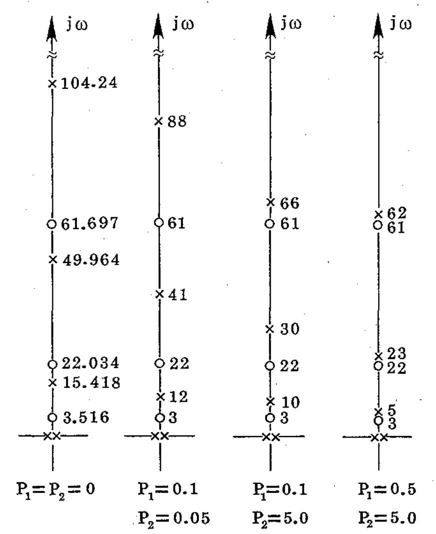

Fig. 2 Exact poles and zeros of $\theta(s)/u(s)$ for different values of structual parameters.

where $z(x,t)$ is transverse displacement of the membrane; ρ_0 is mass density per unit area of the membrane; and T_0 is tension per unit length. The boundary conditions for pure roll motion are

$$z(l,t) = l\phi(t), \qquad z(0,t) = 0 \tag{9}$$

where $\phi(t)$ is the attitude angle of the rigid frame and $2l$ is total length of the frame.

The equation of motion of the rigid frame is

$$J\ddot{\phi} = [z'(l,t) + \phi(t)]l(2aT_0) + u(t) \tag{10}$$

where J is rotational inertia of the rigid frame; $u(t)$ is the roll control torque applied to the frame through the rigid shaft; and a is width of the frame. The rotational inertia of the rigid shaft is omitted for simplicity.

Taking the Laplace transform of Eq. (8), we get

$$z''(x,s) + [\lambda^2 z(x,s)] = 0 \tag{11}$$

where $\lambda^2 \triangleq -s^2$, s is in units of $\sqrt{T_0/\rho_0 l^2}$ and z and x are in units of l. Finally, we have the transcendental transfer function from roll control torque $u(s)$ to roll attitude angle $\phi(s)$

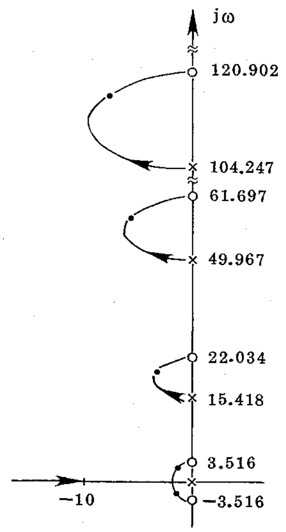

Fig. 3 Exact root locus vs rate feedback gain.

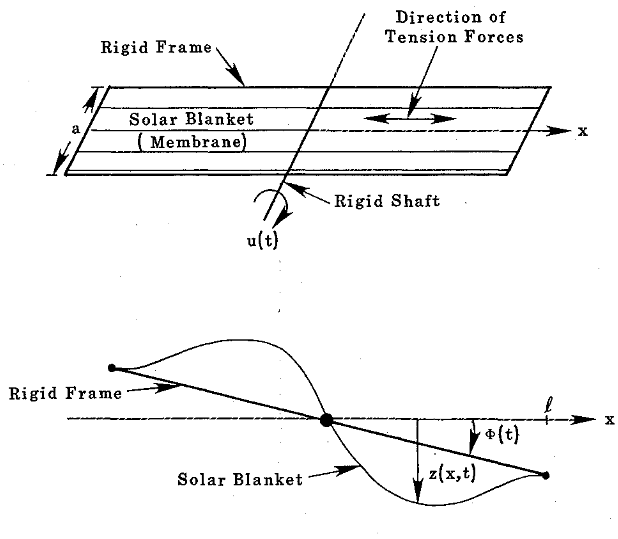

Fig. 4 Rigid frame with a pretensioned membrane.

$$\frac{\phi(s)}{u(s)} = \frac{\sin\lambda}{aT_0 l\left[(3/2)r\lambda^2 \sin\lambda - 2(\sin\lambda + \lambda\cos\lambda)\right]} \quad (12)$$

where

$$r = \frac{J}{(2/3)a\rho_0 l^3} = \frac{\text{moment of inertia of rigid frame}}{\text{moment of inertia of solar blanket}}$$

As $\lambda \to 0$, Eq. (12) becomes

$$\frac{\phi(s)}{u(s)} = \frac{1}{\left[J + (2/3)a\rho_0 l^3\right]s^2} \quad (13)$$

which is identical to the transfer function of a rigid frame with a rigid solar blanket.

The numerator of Eq. (12) is identical to the characteristic equation of a vibrating string of length l. The pole-zero patterns of Eq. (12) are shown in Fig. 5 for different values of inertia ratio r. As $r \to \infty$, we have near pole-zero cancellations of vibration modes, which means that the membrane vibration becomes negligible and the entire system behaves as a rigid body.

Flexible Frame with a Pretensioned Membrane

Consider a simple model of a flexible frame with a pretensioned membrane, as shown in Fig. 6. The equation of motion for the solar blanket is identical to Eq. (8)

$$z''(x,t) - \left[(\rho_0/T_0)\ddot{z}(x,t)\right] = 0$$

with boundary conditions for pure roll motion

$$z(0,t) = 0, \qquad z(l,t) = y(l,t) \quad (14)$$

where $z(x,t)$ is the transverse displacement of solar blanket, $y(x,t)$ is the transverse displacement of the support boom, and ρ_0 and T_0 are as defined in the previous section.

Since the support booms are compressed, due to the tension in the solar blanket, they are described by beam-column equations

$$EIy''''(x,t) + \left[(aT_0/2)y''(x,t)\right] + \left[\sigma_0 \ddot{y}(x,t)\right] = 0 \quad (15)$$

With boundary conditions

$$4EIy''(0,t) = u(t) \quad \text{and} \quad y(0,t) = y''(l,t) = 0 \quad (16)$$

EI represents the bending stiffness of support booms, σ_0 is the mass per unit length of booms, and $u(t)$ is roll control torque applied through the rigid shaft. For the tip rigid bar, we have

$$m_0\ddot{y}(l,t) - \left[2EIy'''(l,t)\right] - \left[aT_0 y'(l,t)\right] + \left[aT_0 z'(l,t)\right] = 0 \quad (17)$$

The Laplace transforms of the above equations of motion and the boundary conditions can be written in dimensionless form as follows:

Solar Blanket: $z'' + \left[\lambda^2 z(x,s)\right] = 0 \quad (18)$

Beam Column: $y'''' + Ty'' - \left[\sigma T\lambda^2 y(x,s)\right] = 0 \quad (19)$

Tip Bar: $-m\lambda^2 y(1,s) - \left[(1/T)y'''(1,s)\right] - \left[y'(1,s)\right] + \left[z'(1,s)\right] = 0 \quad (20)$

Boundary Conditions:

$$z(0,s) = 0,\ z(1,s) = y(1,s),\ y(0,s) = 0,$$
$$y''(1,s) = 0,\ 4y''(0,s) = u(s) \quad (21)$$

where $\lambda^2 \triangleq -s^2$ (s in units of $\sqrt{T_0/\rho_o l^2}$), x, y and z are in units of l, and $u(s)$ is in units of EI/l. The dimensionless structural parameters m, σ, and T are defined as

$$m = \frac{m_0}{a\rho_0 l} = \frac{\text{mass of tip rigid bar}}{\text{mass of solar blanket (one side)}} \quad (22a)$$

$$\sigma = \frac{2\sigma_0 l}{a\rho_o l} = \frac{\text{mass of support booms (one side)}}{\text{mass of solar blanket (one side)}} \quad (22b)$$

$$T = \frac{aT_0 l^2}{2EI} = \pi^2 \frac{\text{compressive load} \triangleq (aT_0/2)}{\text{buckling load} \triangleq (1/\pi^2)(EI/l^2)} \quad (22c)$$

The solution of Eq. (19) is given as

$$y(x,s) = B_1 sh\alpha x + B_2 ch\alpha x + B_3 s\beta x + B_4 c\beta x \quad (23)$$

where

$$\alpha \triangleq \left[\frac{-T + \sqrt{T^2 + 4\sigma T\lambda^2}}{2}\right]^{1/2}$$

$$\beta \triangleq \left[\frac{T + \sqrt{T^2 + 4\sigma T\lambda^2}}{2}\right]^{1/2}$$

The transcendental transfer function from control torque $u(s)$ to roll attitude angle $\phi(s) \triangleq y'(0,s)$ can then be found as

$$\frac{\phi(s)}{u(s)} = \frac{\alpha(b_1 a_{22} - b_2 a_{12}) + \beta(b_2 a_{11} - b_1 a_{21})}{a_{11}a_{22} - a_{12}a_{22}} \quad (24)$$

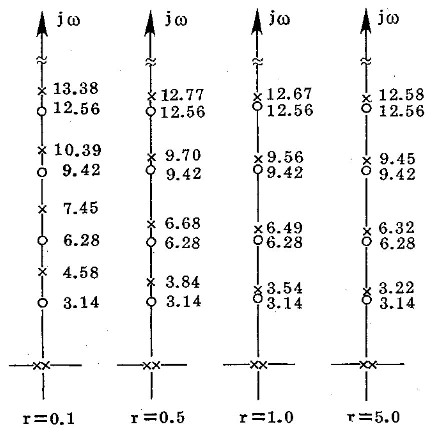

Fig. 5 Exact poles and zeros of the roll transfer function (r = the moment of inertia ratio).

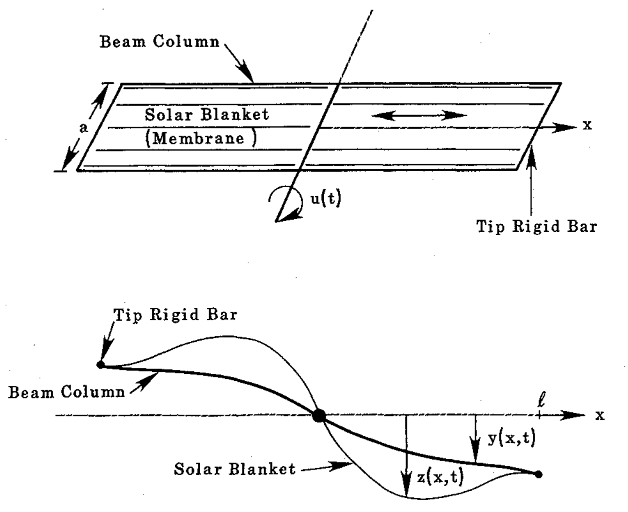

Fig. 6 Flexible frame with a pretensioned membrane.

where

$$a_{11} = (\alpha^2 sh\alpha)(\alpha^2+\beta^2)$$
$$a_{12} = -\beta^2 s\beta(\alpha^2+\beta^2)$$
$$a_{21} = (\alpha^2+\beta^2)[(-m\lambda^2 s\lambda + \lambda c\lambda)sh\alpha - (\alpha^2 ch\alpha/T - \alpha ch\alpha)s\lambda]$$
$$a_{22} = (\alpha^2+\beta^2)[(-m\lambda^2 s\lambda + \lambda c\lambda)s\beta + (\beta^3 c\beta/T - \beta c\beta)s\lambda]$$
$$b_1 = -(\alpha^2 ch\alpha + \beta^2 c\beta)/4$$
$$b_2 = [-(-m\lambda^2 s\lambda + \lambda c\lambda)(ch\alpha - c\beta) + (\alpha^3 sh\alpha - \beta^3 s\beta)s\lambda/T + (\alpha sh\alpha + \beta s\beta)s\lambda]/4$$

The exact pole-zero patterns of Eq. (24) are shown in Fig. 7 for different values of T. The nominal values are assumed as: $m=0.2$, $\sigma=0.2$, and $T=2.0$. The lowest poles and zeros approach the origin as $T\to\pi^2$, i.e., $aT_0/2\to$ buckling load $(EI/\pi^2 l^2)$. For the nominal value of $T=2.0$, each pole has an associated zero of higher frequency than the pole with near cancellation. The lowest zeros are quite close to the origin. Thus the reduced-order models obtained from the product expansion of transcendental transfer function will have the same number of poles and zeros, while the reduced-order models obtained by modal analysis have always more poles than zeros. Most physical systems are "strictly proper" systems, which have more poles than zeros in the transfer functions. However, some dynamic systems, such as the generic examples considered in this paper, behave as "proper" systems with direct transmission. A simple mass-spring model with such direct transmission characteristics can be found in Refs. 12 and 13.

An Equilateral Triangular Truss

It is possible to determine exact transfer functions for structures built-up from several beams. This method is applied to a generic planar structure made up of three beams forming an equilateral triangle. Unlike one-dimensional structures (e.g., a single beam), a planar structure can have repeated natural frequencies, a source of concern to control designers. With three identical beam elements, the generic planar structure considered here has many repeated natural frequencies.

Using the symmetry of the triangular structure (Fig. 8), actuators and sensors can be placed so that roll, pitch, and yaw can be controlled independently. It is straightforward to find exact transfer functions from one end of a beam to the other for displacement, slope, moment, and shear (see Appendix). Roll-axis modeling using a transfer-matrix description of a uniform beam (Eq. A1) is discussed here; pitch- and yaw-axis modeling can be found in Refs. 12 and 15.

For roll attitude control, we place a torquer (e.g., a reaction wheel) and an attitude sensor (or rate gyro) at the center of the rear beam. From the anti-symmetry of the motions, we need only consider half of the structure, e.g., the right half (Fig. 8). We assume all three beams have bending stiffness EI, mass per unit length σ, and length $2l$. The moment Q_1 is half of the control torque $(-Q_R/2)$. The slope of the beam at the center θ_1 is the sensed quantity (ϕ). The anti-symmetry of the roll motions requires that the displacement y_1 and y_4 be zero. The displacements y_2 and y_3 and the shear forces F_2 and F_3 must be equal. Assuming "ball-in-socket" joints, the moments Q_2, Q_3, and Q_4 must be zero. For rigid joints, one must consider torsion of the beam elements, since bending moments at the end of one beam element produce both bending moment and torsion in the next beam element. This triangular frame is treated in Ref. 12.

Using these eight conditions with the eight equations of the two transfer matrices yields the following transfer function from Q_R to ϕ

$$\frac{\phi(s)}{Q_R(s)} = \frac{N(s)}{D(s)} \tag{25}$$

where

$\phi(s)$ = roll attitude angle ($= -\theta_1$ in Fig. 8)

$Q_R(s)$ = roll control torque ($= -2Q_1$ in Fig. 8)

s = Laplace transform variable in units of $\sqrt{EI\sigma^3/l^2}$

$$\lambda^4 = (-s)^2$$
$$N(s) = (ch2\lambda s2\lambda - sh2\lambda c2\lambda)(ch\lambda s\lambda - sh\lambda c\lambda)/4 - sh2\lambda s2\lambda(1+ch\lambda c\lambda)/2$$
$$D(s) = sh\lambda s\lambda(ch2\lambda s2\lambda - sh2\lambda c2\lambda) + sh2\lambda s2\lambda(ch\lambda s\lambda - sh\lambda c\lambda)$$

Equation (25) may be written in an infinite product expansion form in dimensional units

$$\frac{\phi(s)}{Q_R(s)} = \frac{1}{Js^2}\prod_{i=1}^{\infty}\frac{s^2/z_i^2+1}{s^2/p_i^2+1} \tag{26}$$

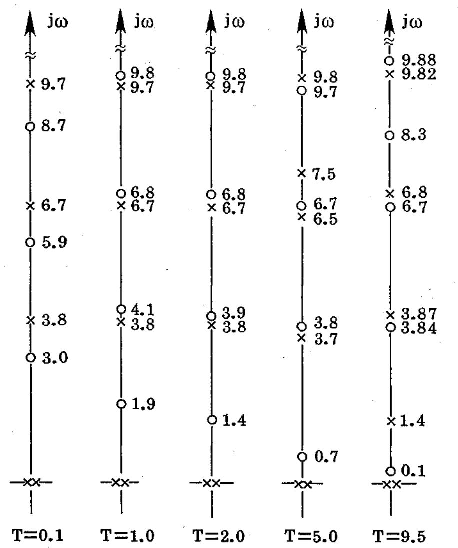

Fig. 7 Exact poles and zeros with $m=\sigma=0.2$.

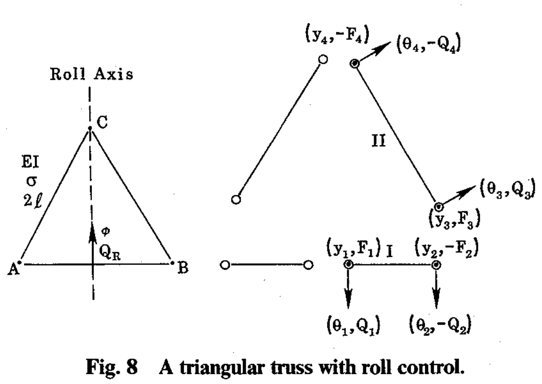

Fig. 8 A triangular truss with roll control.

where $J = 2\sigma l^3$ represents roll moment of inertia of the rigid truss, p_i is the ith pole, and z_i is the ith zero. The exact poles and zeros of the roll transfer function for the lowest few modes are shown in Fig. 9a. From this figure, we see that poles and zeros alternate with near pole-zero cancellations of modes, 1, 2, 4, and 5. Again, one of the unique characteristics of this pole-zero pattern is that each pole has an associated zero of higher frequency than the pole.

Pitch-axis modeling can be performed in a manner similar to the roll-axis modeling.[12,15] Two identical torquers are placed at the centers of the side beams. Two identical sensors are also placed similarly. The exact poles and zeros of the pitch transfer function for the lowest few modes are shown in Fig. 9b. The plunge modes, which cannot be observed or controlled by the pitch sensors and torquers, have exact pole-zero cancellations in the pitch channel. The pitch modes have the same natural frequencies as those of roll modes, except for the 2nd and 5th roll modes. Such repeated natural frequencies are due to the symmetry of the triangular truss. Consequently, the pitch rigid inertia is the same as the roll rigid inertia (any orthogonal axes on the roll/pitch plane of the equilateral triangular truss are principal axes).

An exact root locus vs. rate feedback gain for the roll axis is shown in Fig. 10. It is clear from the figure that each pole has an associated zero of higher frequency than the pole, and that the 3rd and 6th flexible modes are the dominant modes in roll axis. This exact root locus indicates that the closed-loop behavior observed in Fig. 3 for one-dimensional structures can also be observed for a planar structure.

Some Practical Issues

Thus far, we have considered the pole-zero modeling of some generic models of flexible structures. In particular, we determined the exact transfer functions form applied torques to attitude angles at the points where the control torquers are located. Although analytical frequency-domain modeling of some hybrid systems was possible, the derivation of exact transfer functions involved a fair amount of effort. Perhaps a more logical next step will be the development of a computer-aided approach to the frequency-domain modeling of hybrid systems with complex interconnections of lumped and beam- or truss-like lattice substructures. Consequently, various algorithms and techniques for numerical or symbolic manipulation of frequency-domain continuum models are under development.[4-8] The various hybrid models considered in this paper will, therefore, be useful for checking or validating the computer-aided techniques so that the practical use of these techniques can be made with confidence to future large space structures.

The practical significance of the pole-zero pattern discussed in this paper is further emphasized here. Figure 11a shows the poles and zeros of reduced-order transfer functions obtained from a finite-element model of the dual-keel Space Station shown in Fig. 11b.[11] These are the transfer function poles and zeros of the colocated actuators (control moment gyros) and sensors in each axis. One very important observation for these transfer functions of the dual-keel Space Station is that the lowest zeros of roll and pitch axes are very close to the origin and that each mode has an associated zero of higher frequency than the pole. This results in a significant pole-zero separation for the dominant flexible modes in the roll/pitch axes. In fact, that is the pole-zero pattern of the simple generic models investigated in this paper.

In this section, we briefly discuss the practical control design issues related to such pole-zero patterns. It is well known that a control logic, which is a direct feedback of position and rate, and is designed to stabilize the rigid body mode, naturally stabilizes all the flexible modes when the actuator and sensor are colocated.[9,10] However, as discussed in Refs. 11, 16 and 17, phase stabilization of all the flexible modes may not be practical in the presence of the

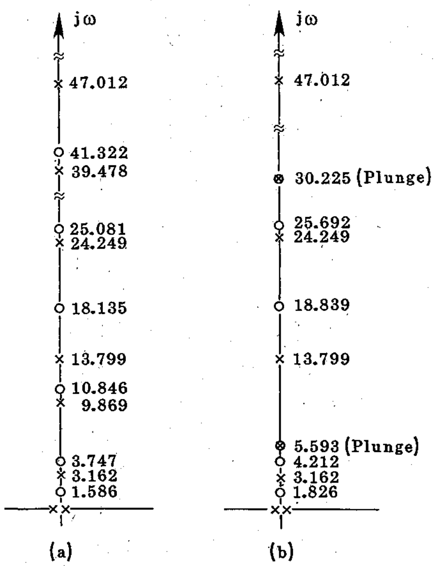

Fig. 9 Exact poles and zeros: (a) roll; (b) pitch.

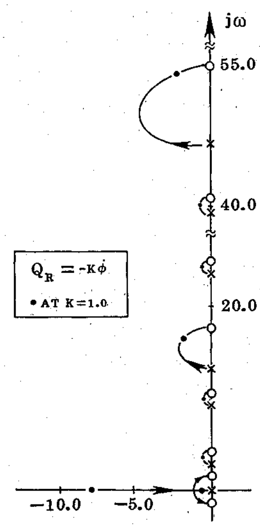

Fig. 10 Exact root locus vs rate feedback gain.

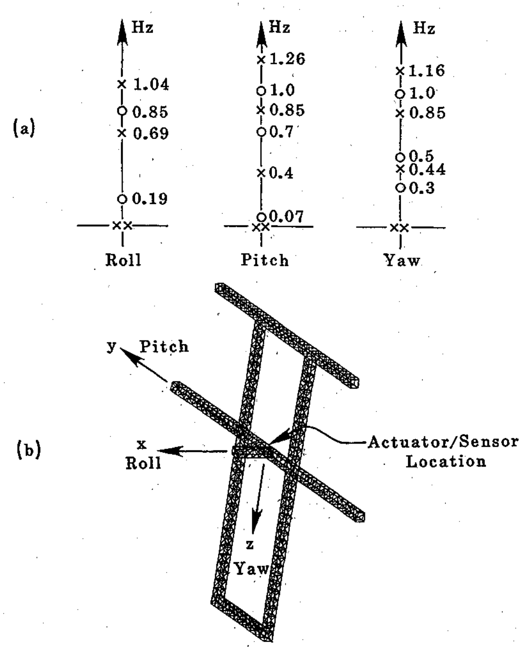

Fig. 11 Poles and zeros of the reduced-order transfer functions of the dual keel space station.

actuator/sensor dynamics and the control loop time delay. In practice, the dominant flexible modes are usually phase stabilized and all the higher-frequency modes are gain stabilized. Passive damping becomes critical for gain stabilization, while it is not critical for phase stabilization. The phase stabilization of dominant flexible modes by the attitude control logic needs great care when the dominant mode frequency is relatively high and when the lowest zeros are very close to the origin.[11,16]

As demonstrated experimentally in Ref. 18, controlling a flexible structure using a noncolocated actuator/sensor pair is a difficult control problem. It is now generally accepted that the colocated control is a rather simple problem when compared to the noncolocated control. It is, however, emphasized that the colocated control of flexible structures with a direct transmission characteristic (such as the generic models discussed in this paper and the dual-keel Space Station) is not a trivial problem, if a high bandwidth control is required. As a result, a combination of the modified LQG synthesis technique[19] and the enhanced classical control synthesis techniques[20-21] is under investigation for robust structural filtering of flexible structures which have direct transmission characteristics.

Conclusions

We have described the "exact" frequency-domain modeling of some generic models of flexible space structures. These models are simple enough to treat analytically, yet complicated enough to demonstrate the practical usefulness of frequency-domain modeling. A feature of transfer functions derived in this manner is that each pole has an associated zero of higher frequency. The dual-keel Space Station has a pole-zero pattern very similar to those of the generic models developed in this paper. Such pole-zero patterns must be carefully considered when designing large space platforms and placing actuators and sensors. We hope that the physical insights obtained by investigating these simple hybrid models will be useful in analyzing large space structures with complex interconnections of lumped and distributed parameter subsystems.

Appendix

Matrix Descriptions of a Uniform Beam

Consider a uniform Bernoulli-Euler beam with forces and torques acting only on the two ends of the beam. The Laplace-transformed equation of motion is

$$y''''(x,s) - \lambda^4 y(x,s) = 0$$

and its solution is given by

$$y(x,s) = A_1 \sin\lambda x + A_2 \cos\lambda x + A_3 \sinh\lambda x + A_4 \cosh\lambda x.$$

The three different matrix descriptions (transfer matrix, impedance matrix, and admittance matrix) are summarized as follows:

A1 Transfer Matrix

$$\begin{bmatrix} y_2 \\ \theta_2 \\ -Q_2 \\ F_2 \end{bmatrix} = \begin{bmatrix} T_1 & T_2 & T_3 & T_4 \\ T_4 & T_1 & T_2 & T_3 \\ T_3 & T_4 & T_1 & T_2 \\ T_2 & T_3 & T_4 & T_1 \end{bmatrix} \begin{bmatrix} y_1 \\ \theta_1 \\ -Q_1 \\ F_1 \end{bmatrix} \tag{A1}$$

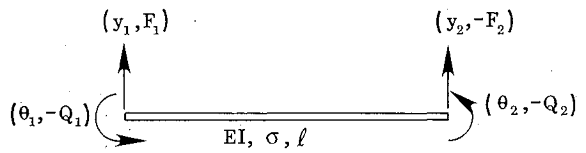

Fig. A1 Sign connection for the transfer matrix.

where

y_i = bending displacement in units of l (see Fig. A1)

θ_i = bending slope in units of λ

Q_i = bending moment in units of $EI\lambda^2/l$

F_i = shear force in units of $EI\lambda^3/l^2$

$\lambda^2 = -s^2$

s = Laplace transform variable in units of $\sqrt{EI/\sigma l^4}$

$$T_{1,3}(\lambda) = \tfrac{1}{2}(\cosh\lambda \pm \cos\lambda)$$

$$T_{2,4}(\lambda) = \tfrac{1}{2}(\sinh\lambda \pm \sin\lambda)$$

A2 Impedance (Dynamic Stiffness) Matrix

$$\begin{bmatrix} -1 & 0 & 1 & 0 \\ c\lambda & -s\lambda & -ch\lambda & -sh\lambda \\ 0 & 1 & 0 & -1 \\ -s\lambda & -c\lambda & sh\lambda & ch\lambda \end{bmatrix} \times \begin{bmatrix} 0 & 1 & 0 & 1 \\ s\lambda & c\lambda & sh\lambda & ch\lambda \\ 1 & 0 & 1 & 0 \\ c\lambda & -s\lambda & ch\lambda & sh\lambda \end{bmatrix}^{-1} \times \begin{bmatrix} y_1 \\ y_2 \\ \theta_1 \\ \theta_2 \end{bmatrix} = \begin{bmatrix} F_1 \\ F_2 \\ Q_1 \\ Q_2 \end{bmatrix} \tag{A2}$$

$$\Rightarrow \frac{1}{1 - c\lambda ch\lambda} \begin{bmatrix} K_1 & K_2 & K_3 & K_4 \\ K_2 & K_1 & -K_4 & -K_3 \\ K_3 & -K_4 & K_5 & K_6 \\ K_4 & -K_3 & K_6 & K_5 \end{bmatrix} \times \begin{bmatrix} y_1 \\ y_2 \\ \theta_1 \\ \theta_2 \end{bmatrix} = \begin{bmatrix} F_1 \\ F_2 \\ Q_1 \\ Q_2 \end{bmatrix} \tag{A3}$$

where $K_1 = s\lambda ch\lambda + c\lambda sh\lambda$, $K_2 = -(s\lambda + sh\lambda)$, $K_3 = s\lambda sh\lambda$, $K_4 = ch\lambda - c\lambda$, $K_5 = s\lambda ch\lambda - c\lambda sh\lambda$, $K_6 = sh\lambda - s\lambda$; y_i, θ_i, Q_i and F_i are the same as defined in Eq. (A1) except the sign convention shown in Fig. A2.

A3 Admittance (Dynamic Flexibility) Matrix

$$\begin{bmatrix} y_1 \\ y_2 \\ \theta_1 \\ \theta_2 \end{bmatrix} = \begin{bmatrix} 0 & 1 & 0 & 1 \\ s\lambda & c\lambda & sh\lambda & ch\lambda \\ 1 & 0 & 1 & 0 \\ c\lambda & -s\lambda & ch\lambda & sh\lambda \end{bmatrix} \times \begin{bmatrix} -1 & 0 & 1 & 0 \\ c\lambda & -s\lambda & -ch\lambda & -sh\lambda \\ 0 & 1 & 0 & 1 \\ -s\lambda & -c\lambda & sh\lambda & ch\lambda \end{bmatrix}^{-1} \begin{bmatrix} F_1 \\ F_2 \\ Q_1 \\ Q_2 \end{bmatrix} \tag{A4}$$

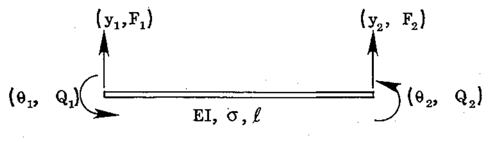

Fig. A2 Sign connection for the impedence and admittance matrices.

$$\Rightarrow \begin{bmatrix} y_1 \\ y_2 \\ \theta_1 \\ \theta_2 \end{bmatrix} = \frac{1}{1 - c\lambda ch\lambda} \begin{bmatrix} -K_5 & K_6 & K_3 & K_4 \\ K_6 & -K_5 & -K_4 & -K_3 \\ K_3 & -K_4 & -K_1 & K_2 \\ K_4 & -K_3 & K_2 & -K_1 \end{bmatrix} \times \begin{bmatrix} F_1 \\ F_2 \\ Q_1 \\ Q_2 \end{bmatrix} \tag{A5}$$

where K_i are the same as defined in Eq. (A2); y_i, θ_i, Q_i and F_i are as defined in Eq. (A1), except the sign convention shown in Fig. A2.

References

[1]Noor, A.K., Anderson, M.S., and Green, W.H., "Continuum Models for Beam- and Plate-Like Lattice Structures," *AIAA Journal*, Vol. 16, No. 12, Dec. 1978, pp. 1219–1228.

[2]Nayfeh, A. and Hefzy, M.S., "Continuum Modeling of Three-Dimensional Truss-Like Space Structures," *AIAA Journal*, Vol. 16, 1978, pp. 779–787.

[3]Renton, J.D., "The Beam-Like Behavior of Space Trusses," *AIAA Journal*, Vol. 22, 1984, pp. 273–280.

[4]Blankenship, G.L., "Homogenization and Control of Lattice Structures," Proc. 5th VPI&SU/AIAA Symposium on Dynamics and Control of Large Structures, June 1985.

[5]Bennett, W.H. et al., "Continuum Modeling of Lattice Structures with Application to Vibration Control," AIAA Paper 86-0173, Jan. 1986.

[6]Bennett, W.H. and Barkakati, N., "FlexCAD: Prototype Software for Modeling and Control of Flexible Structures," presented at IEEE CACSD Symposium, Sept. 1986.

[7]Poelaert, D., "DISTEL: A Distributed Element Program for Dynamic Modeling and Response Analysis of Flexible Structures," *Proceedings of 4th VPI&SU/AIAA Symposium on Large Structures,* AIAA, New York, 1983.

[8]Piche, R., "Frequency-Domain Continuum Modeling and Control of Third-Generation Spacecraft," TR Waterloo Research Institute, University of Waterloo, Canada, 1985.

[9]Gevarter, W.B., "Basic Relations for Control of Flexible Vehicles," *AIAA Journal*, Vol. 8, April 1970.

[10]Martin, G.D. and Bryson, A.E. Jr., "Attitude Control of a Flexible Spacecraft," *Journal of Guidance, Control, and Dynamics*, Vol. 3, No. 1, Jan.–Feb. 1980, pp.

[11]Chu, P., Wie, B., Gretz, B., and Plescia, C., "Space Station Attitude Control: Modeling and Design," AIAA Guidance, Navigation, and Control Conference, Aug. 15–17, 1988 (to be presented).

[12]Wie, B., "On the Modeling and Control of Flexible Space Structures," SUDAAR 525, Ph.D. Thesis, Stanford University, Stanford, CA, 1981.

[13]Wie, B. and Bryson, A.E., Jr., "Modeling and Control of Flexible Space Structures," *Proceedings of 3rd VPI&SU/AIAA Symposium on the Dynamics and Control of Large Flexible Space Structures,* AIAA, New York, 1981, pp. 153–174.

[14]Wie, B., "Active Vibration Control Synthesis for the COFS-I: A Classical Approach," AIAA Paper 87-2322, Aug. 1987.

[15]Wie, B. and Bryson A.E. Jr., "Attitude Control of a Triangular Truss in Space," IFAC 8th World Congress, Paper 77-2, Kyoto, Japan, Aug. 1981.

[16]Wie, B. and Plescia, C.T., "Attitude Stabilization of a Flexible Spacecraft During Stationkeeping Maneuvers," *Journal of Guidance, Control, and Dynamics*, Vol. 7, No. 4, July–Aug. 1984, pp. 430–436.

[17]Wie, B., Lehner, J.A., and Plescia, C.T., "Roll/Yaw Control of a Flexible Spacecraft Using Skewed Bias Momentum Wheels," *Journal of Guidance, Control, and Dynamics*, Vol. 8, No. 4, July–Aug. 1985, pp. 447–453.

[18]Cannon, R.H. Jr. and Rosenthal, D.E., "Experiments in Control of Flexible Structures with Noncolocated Sensors and Actuators," *Journal of Guidance, Control, and Dynamics*, Vol. 7, No. 5, Sept.–Oct. 1984, pp. 546–553.

[19]Bryson, A.E. Jr., et al., "LQG Controller Design for Robustness," presented at the 1986 American Control Conference, Seattle, WA, June 1986.

[20]Wie, B. and Byun, K.W., "A New Concept of Generalized Structural Filtering for Active Vibration Control Synthesis," AIAA Paper 87-2456, Aug. 1987.

[21]Wie, B. and Bryson, A.E. Jr., "On Multivariable Control Robustness Examples: A Classical Approach," *Journal of Guidance, Control, and Dynamics*, Vol. 10, No. 1, Jan.–Feb. 1987, pp. 118–120.